Applied Surface Science 261 (2012) 123–127

Contents lists available at SciVerse ScienceDirect

Applied Surface Science

journal homepage: www.elsevier.com/locate/apsusc

Near ultraviolet photodetector fabricated from polyvinyl-alcohol coated In_2O_3 nanoparticles

Dali Shao*, Liqiao Qin, Shayla Sawyer

Electrical, Computer, and Systems Engineering Department, Rensselaer Polytechnic Institute, Troy, NY 12180, USA

ARTICLE INFO

Article history:
Received 20 July 2012
Accepted 21 July 2012
Available online 14 August 2012

Keywords:
PVA coated In_2O_3 nanoparticles
Near UV
Surface oxygen vacancy defects
Enhanced photoresponsivity

ABSTRACT

A near ultraviolet (UV) photodetector is fabricated from colloidal In_2O_3 nanoparticles coated with polyvinyl-alcohol (PVA). The device exhibits lower dark current and higher responsivity compared with a photodetector fabricated from uncoated In_2O_3 nanoparticles. The rise and fall time of the PVA coated photodetector is about 500 s and 1600 s, respectively, one half of the uncoated device. The faster response time of the PVA enhanced photodetector is due to surface passivation which reduces the surface defects while enhancing desorption of oxygen from the nanoparticle surface, thus increasing free carrier concentration.

1. Introduction

In wide band-gap semiconductor materials, In_2O_3 has been investigated extensively for its promising applications including: field effect transistors (FET) [1–5], gas sensing [6–9] and optoelectronic devices [10–12]. UV photodetectors based on wide band gap semiconductors such as GaN, ZnO, TiO_2 and diamond [13–19] have been widely reported, only a few were created with In_2O_3 nanoparticles [23]. Here, we report the fabrication of metal–semiconductor–metal (MSM) near-UV photodetector by spin-coating polyvinyl-alcohol (PVA) coated In_2O_3 nanoparticles onto quartz substrates. To our knowledge, this is the first demonstration of a near-UV photodetector fabricated from solution processed In_2O_3 colloidal nanoparticles on quartz substrates.

2. Experimental details

The photodetectors were fabricated from commercial In_2O_3 nanoparticles (US Research Nanomaterials Inc.) with a purity of 99.995% and sizes ranging from 20 to 70 nm. Two batches of In_2O_3 nanoparticles were prepared. The first batch was dispersed in ethanol to form 40 mg/ml suspension. For the second batch, the In_2O_3 nanoparticles were surface treated with PVA solutions (1% in weight in water), which provide surface passivation. Then they were centrifuged and dispersed in ethanol. The concentration of the suspension was also 40 mg/ml. These solutions were then spin-coated onto quartz substrate and annealed in air at 120 °C for 5 min, respectively. High resolution scanning electron microscope (SEM) image was taken by a Carl Zeiss Ultra 1540 dual beam SEM, as shown in Fig. 1(a). The photodetectors were fabricated by thermally depositing 250 nm interdigitated aluminum (Al) contacts on top of the In_2O_3 nanoparticles. The deposition of Al was done using E-beam evaporation through a shadow mask. Finally, the photodetectors were packaged and wire bonded utilizing Epo-Tek H20E conductive epoxy. The 3D view of the fabricated photodetector is shown in Fig. 1(b).

3. Results and discussion

The dark current and photocurrent of the photodetectors fabricated from PVA coated and uncoated In_2O_3 nanoparticles are shown in Fig. 2(a) and (b), which were measured using a HP4155B semiconductor parameter analyzer under darkness and under illumination by a 335 nm UV LED with intensity of 31.65 mW/cm^2. The nonlinear IV curves suggest Schottky contacts are formed between Al and PVA coated In_2O_3. Since the electron affinity of In_2O_3 is 3.7 eV, which is lower than the work function of Al (4.08 eV), the formation Schottky contacts is possible. When biased at 20 V, the dark current of the PVA coated photodetector is about one fifth of the uncoated photodetector, while the photocurrent is about 2.5 times of the uncoated sample, thus leading to a higher photocurrent to dark current ratio (shown in Fig. 2(c)). The lower dark current of the PVA coated photodetector is likely attributed to the change of the Schottky barrier height between the interface of Al and In_2O_3

* Corresponding author.
E-mail address: shaodali828@gmail.com (D. Shao).

0169-4332/$ – see front matter © 2012 Elsevier B.V. All rights reserved.
http://dx.doi.org/10.1016/j.apsusc.2012.07.111

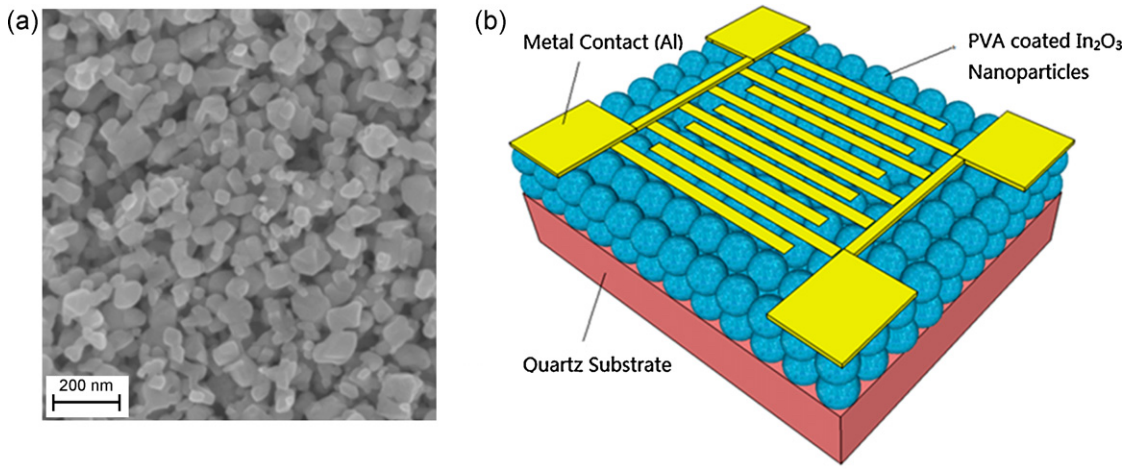

Fig. 1. (a) High resolution SEM image of PVA coated In_2O_3 nanoparticles. (b) 3D view of the photodetector fabricated from PVA coated In_2O_3 nanoparticles (not to scale). The Al contacts on the top are interdigitated finger pattern.

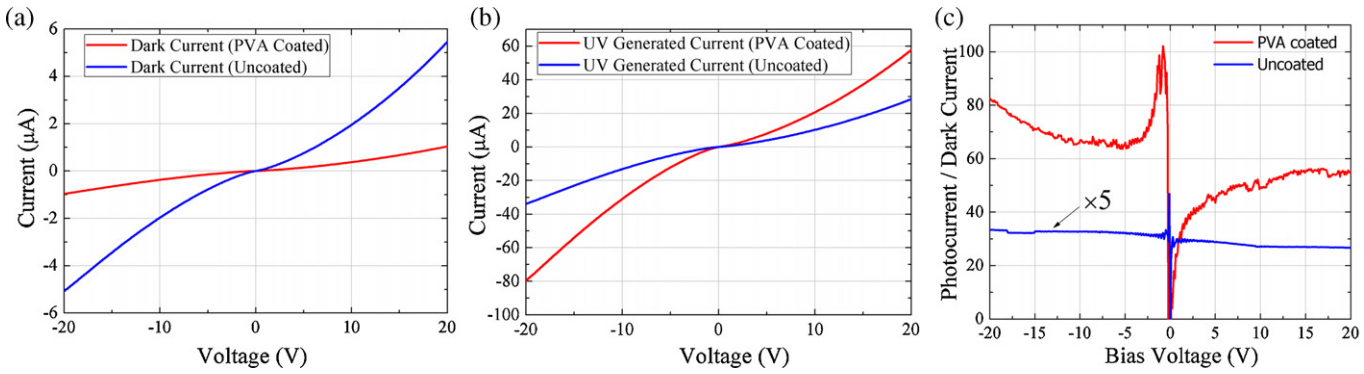

Fig. 2. (a) Dark current, (b) photocurrent and inset: ratio of UV generated current to dark current of photodetectors based on PVA coated and uncoated In_2O_3 nanoparticles, respectively.

nanoparticles, as shown in Fig. 3(a). According to the conventional description of the Schottky UV detector, dark *I–V* characteristics in the thermionic-field emission regime follow the known relation [20,21]:

$$I_{\text{dark}} = I_0 \exp\left(-\frac{q\phi_b}{kT}\right) \exp\left(\frac{qV}{kT} - 1\right)$$

where I_0 is a constant, q is the electron charge, kT is the thermal energy, and ϕ_b is the Schottky barrier height. So it is possible that PVA modified the density of defect states on the surface of the In_2O_3 nanoparticles and hence increased the barrier height. Taking the image force into consideration, the real barrier will be lowered by $\Delta\phi$, which is defined as:

$$\Delta\phi = \left[\frac{q^3 N|\Psi_s|}{8\pi^2\varepsilon_s^3}\right]^{1/4}$$

where N is the dopant concentration, Ψ_s is the surface potential, and ε_s is the permittivity of the semiconductor. Thus, the lower dark current can also be explained as the reduction of surface potential due to PVA, which in turn leads to lower $\Delta\phi$ and therefore higher real barrier height.

To study the photogenerated current of In_2O_3 film, it is important to know the two major mechanisms that are active in the In_2O_3 film (shown in Fig. 3(b)). There are four primary steps to describe the current contributions. First, because of the affinity between the oxygen molecules and electrons, oxygen molecules adsorb onto In_2O_3 surface and capture nearby electrons to form an O_2^- layer [$O_2(g) + e^- \rightarrow O_2^-(ad)$], which leads to a formation of depletion region near the surface and a decrease of free carrier concentration. This oxygen adsorption usually happens on the surface oxygen vacancy sites, common to In_2O_3 nanoparticles because of incomplete oxidation and imperfect crystallization. Several theoretical predictions indicate that surface defects such as oxygen vacancies often dominate the electronic/chemical properties and adsorption behaviors of metal oxide surfaces [33,34]. Thus, for thin films fabricated from nanoparticles, oxygen adsorption processes dominate and the depletion region can extend throughout the entire film due to the high surface to volume ratio.

Second, upon exposure to UV light, the oxygen ions will recombine with the photogenerated holes and therefore desorb oxygen from the surface of In_2O_3 nanoparticles [$h^+ + O_2^-(ad) \rightarrow O_2(g)$], resulting in a decrease in the width of the depletion region and increase in the free carrier concentration [22,23]. PVA acts as a surface passivation layer by covering some of the surface oxygen vacancy sites, which lead to a decrease in the density of surface oxygen vacancy sites. Therefore the surface

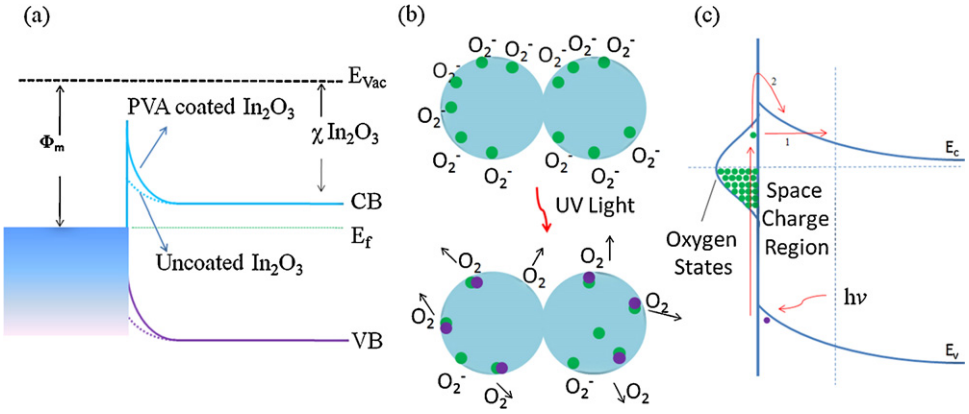

Fig. 3. (a) Schottky barriers formed at the Al/In_2O_3 and Al/PVA–In_2O_3 interfaces. (b) Carrier trapping and transport inside the In_2O_3 nanoparticle film in the dark and under the UV illumination, respectively. (c) Schematic diagram of possible electron transitions under illumination by photons with energy below the fundamental absorption edge with the participation of adsorbed oxygen: (1) tunneling transition from oxygen states to the conduction band; (2) thermally activated transition over the potential barrier (green dots: electrons and purple dots: holes). (For interpretation of the references to color in this figure legend, the reader is referred to the web version of the article.)

oxygen adsorption processes are suppressed, which leads to an increase in the free carrier concentration and enhanced photocurrent in the In_2O_3 film. Moreover, the transport of these free carriers has been modeled as a disordered hopping system. The model explains photocurrent enhancement due to the strong dependence of carrier mobility on free carrier density [29,30].

Third, oxygen vacancy defects usually act as deep defect donors, which lead to parasitic green emissions and can easily trap the photogenerated carriers during their transportation to the contacts [24–28]. Thus, the reduction in the density of surface oxygen vacancy defects means a decrease in the number of carrier trapping centers inside the In_2O_3 film, which also enhance the photocurrent. The decrease in the density of surface oxygen defects for PVA coated In_2O_3 nanoparticles has been confirmed by photoluminescence (PL) measurements on the thin films fabricated from PVA coated and uncoated In_2O_3 nanoparticles. PVA effectively suppresses the parasitic green emission by reducing the surface oxygen vacancy defects. The detailed study of the suppression of green emission for PVA coated In_2O_3 nanoparticles will be presented in another work.

Finally, it is worthy to mention that although the adsorbed oxygen on the nanoparticles surface captures electrons from In_2O_3 films and therefore reduces the free carrier concentration; the adsorbed oxygen indeed can provide some positive effect on photocurrent in another way. As shown in Fig. 3(c), the adsorbed oxygen creates some additional energy states near the conduction band, from which electrons generated by photons with energy below the fundamental states contributing to expanding the absorption edge. Carriers can be collected by either tunneling from oxygen states to the conduction band or by surmounting the potential barrier through thermal activation. However, the carriers generated by surface oxygen assisted transitions are much less than the number of carriers taken away by the surface adsorbed oxygen.

Time resolved photocurrent for PVA coated and uncoated photodetectors are presented in Fig. 4(a) and (b), respectively. The rise time (measured from 10% to 90%) and fall time (from 90% to 10%) for the PVA coated In_2O_3 nanoparticle photodetector are 500 s and 1600 s, respectively. While, for uncoated In_2O_3 nanoparticle photodetector, the rise time is 1100 s and fall time is 3200 s. Since the PVA coated photodetector has a lower density of surface defect states, higher free carrier concentration and higher carrier mobility, a faster time response for rise time is expected. Yet, for fall time, the underlying issue is different. For uncoated devices, after turning off the UV LED, the oxygen will reabsorb to the surface and capture the electrons from the nanoparticle surfaces, which lead to the reduction of current inside the film. Thus we conclude that the faster fall time for PVA coated photodetector is mainly due to the reduction of the surface defects, which outweigh the effect of oxygen reabsorption. In support of

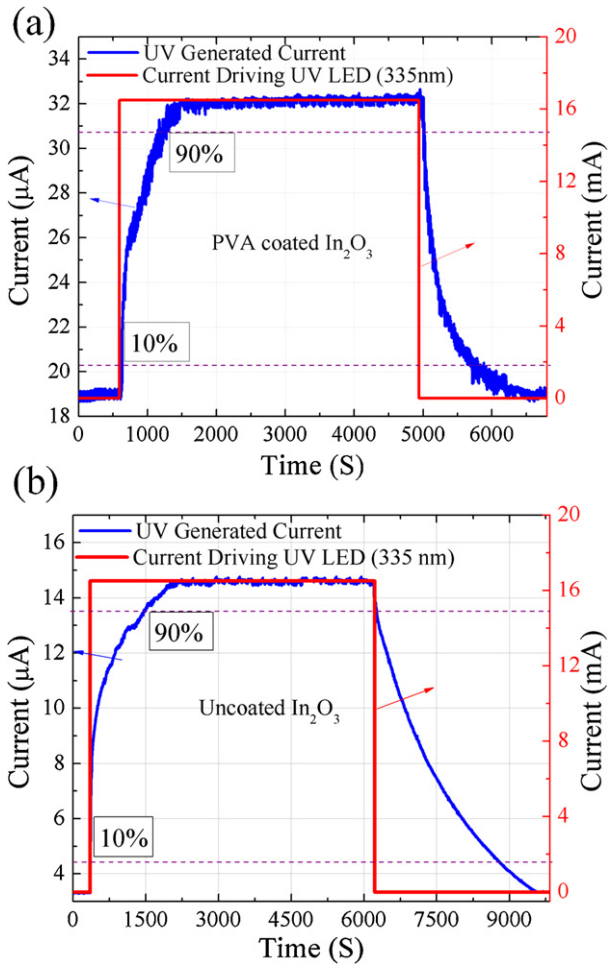

Fig. 4. Time response for photodetector fabricated from (a) PVA coated and (b) uncoated In_2O_3 nanoparticles.

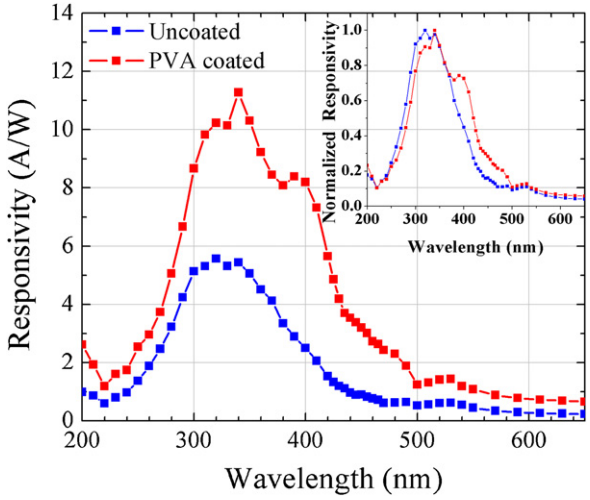

Fig. 5. Photoresponsivity spectra of photodetectors fabricated from PVA coated and uncoated In_2O_3 nanoparticles. The inset is normalized photoresponse spectra.

this conclusion, studies by Zhang et al. [23] proved that NO_2 can significantly reduce the falling time of In_2O_3 nanoparticles, which have a similar but stronger electron capturing effect compared to oxygen.

The responsivity of the devices (shown in Fig. 5), defined as photocurrent per unit of incident optical power, was measured by Shimadzu UV–vis 2550 spectrophotometer with a deuterium lamp (190–390 nm) and a halogen lamp (280–1100 nm). The enhanced responsivity of PVA coated photodetector is attributed to reduced density of surface defects, which have been discussed in previous text. The inset of Fig. 5 is the normalized responsivity for both devices. It shows that after PVA coating, the responsivity spectra red shifted slightly and a new peak at 400 nm appeared. This may be explained by modified surface defect energy levels from PVA, which created new carrier transition paths [31,32].

4. Conclusion

In conclusion, near-UV photodetector fabricated from PVA coated In_2O_3 nanoparticles shows increased photocurrent, suppressed dark current, reduced response time, and altered photoresponse spectra. The mechanisms that contribute to these improvements include: 1. A reduction of the surface oxygen vacancy defects, leading to suppressed surface oxygen adsorption and reduced density of carrier trapping centers. 2. An altered Schottky barrier height. 3. New carrier transition paths created from modifying surface defect energy levels. Future work will focus on additional methods to reduce response time and improve photocurrent to dark current ratio.

Acknowledgements

The authors gratefully acknowledge support from National Security Technologies through NSF Industry/University Cooperative Research Center Connection One. The authors also acknowledge the National Science Foundation Smart Lighting Engineering Research Center (EEC-0812056).

References

[1] A.N. Shipway, E. Katz, I. Willner, Nanoparticle arrays on surfaces for electronic, optical and sensoric applications, ChemPhysChem 1 (2000) 18–52.
[2] F. Favier, E.C. Walter, M.P. Zach, T. Benter, R.M. Penner, Hydrogen sensors and switches from electrodeposited palladium mesowire arrays, Science 293 (2001) 2227–2231.
[3] C. Li, D.H. Zhang, X.L. Liu, S. Han, T. Tang, J. Han, C.W. Zhou, In_2O_3 nanowires as chemical sensors, Applied Physics Letters 82 (2003) 1613–1615.
[4] J. Kong, N.R. Franklin, C.W. Zhou, M.G. Chapline, S. Peng, K.J. Cho, H.J. Dai, Nanotube molecular wires as chemical sensors, Science 287 (2000) 622–625.
[5] A. Kolmakov, M. Moskovits, Chemical sensing and catalysis by one-dimensional metal-oxide nanostructures, Annual Review of Materials Research 34 (2004) 151–180.
[6] G. Korotcenkov, A. Cerneavschi, V. Brinzari, A. Vasiliev, M. Ivanov, A. Cornet, J. Morante, A. Cabot, J. Arbiol, In_2O_3 films deposited by spray pyrolysis as a material for ozone gas sensors, Sensors and Actuators B: Chemical 99 (2003) 297.
[7] M. Ivanovskaya, A. Gurlo, P. Bogdanov, Mechanism of O_3 and NO_2 detection and selectivity of In_2O_3 sensors, Sensors and Actuators B: Chemical 77 (2001) 264–267.
[8] G. Neri, A. Bonavita, G. Micali, G. Rizzo, N. Pinna, M. Niederberger, In_2O_3 and Pt–In_2O_3 nanopowders for low temperature oxygen sensors, Sensors and Actuators B: Chemical 127 (2007) 455–462.
[9] A.Z. Sadek, C. Baker, D.A. Powell, W. Wlodarski, C. Shin, R.B. Kaner, K. Kalantar-zadeh, A polyaniline/In_2O_3 nanofiber composite based layered SAW transducer for gas sensing applications, Nanotechnology 17 (2006) 4488–4492.
[10] L.C. Chen, Indium oxide violet photodiodes, The European Physical Journal – Applied Physics 35 (2006) 13–15.
[11] K.L. Chopra, S. Major, D.K. Pandya, Thin Solid Films 102 (1983) 1–46.
[12] D.S. Ginley, C. Bright, Transparent conducting oxides, MRS Bulletin – Materials Research Society 25 (2000) 15–18.
[13] M.L. Lee, J.K. Sheu, W.C. Lai, Y.K. Su, S.J. Chang, C.J. Kao, C.J. Tun, M.G. Chen, W.H. Chang, G.C. Chi, J.M. Tsai, Characterization of GaN Schottky barrier photodetectors with a low-temperature GaN cap layer, Journal of Applied Physics 94 (2003) 1753–1757.
[14] S.J. Chang, C.L. Yu, C.H. Chen, P.C. Chang, K.C. Huang, Nitride-based ultraviolet metal–semiconductor–metal photodetectors with low-temperature GaN cap layers and Ir/Pt contact electrodes, Journal of Vacuum Science and Technology A 24 (2006) 637–640.
[15] A. Balducci, M. Marinelli, E. Milani, M.E. Morgada, A. Tucciarone, G. Verona-Rinati, M. Angelone, M. Pillon, Extreme ultraviolet single-crystal diamond detectors by chemical vapor deposition, Applied Physics Letters 86 (2005) 193509.
[16] N.W. Emanetoglu, J. Zhu, Y. Chen, J. Zhong, Y. Chen, Y. Lu, Surface acoustic wave ultraviolet photodetectors using epitaxial ZnO, Applied Physics Letters 85 (2004) 3702–3704.
[17] S. Liang, H. Shenga, Y. Liua, Z. Huoa, Y. Lua, H. Shen, ZnO Schottky ultraviolet photodetectors, Journal of Crystal Growth 225 (2001) 110–113.
[18] H. Huang, W. Yang, Y. Xie, X. Chen, Z. Wu, Metal–semiconductor–metal ultraviolet photodetectors based on TiO_2 films deposited by radio-frequency magnetron sputtering, IEEE Electron Device Letters 31 (2010) 588–590.
[19] H. Xue, X. Kong, Z. Liu, C. Liu, J. Zhou, W. Chen, TiO_2 based metal–semiconductor–metal ultraviolet photodetectors, Applied Physics Letters 90 (2007) 201118.
[20] O. Katz, V. Garber, B. Meyler, G. Bahir, J. Salzman, Gain mechanism in GaN Schottky ultraviolet detectors, Applied Physics Letters 79 (2001) 1417–1419.
[21] Y. Xie, H. Huang, W. Yang, Z. Wu, Low dark current metal–semiconductor–metal ultraviolet photodetectors based on sol–gel-derived TiO_2 films, Applied Physics Letters 109 (2011) 023114.
[22] V. Brinzari, M. Ivanov, B.K. Cho, M. Kamei, G. Korotcenkov, Photoconductivity in In_2O_3 nanoscale thin films: interrelation with chemisorbed-type conductometric response towards oxygen, Sensors and Actuators B: Chemical 148 (2010) 427–438.
[23] D. Zhang, C. Li, S. Han, X. Liu, T. Tang, W. Jin, C. Zhou, Ultraviolet photodetection properties of indium oxide nanowires, Applied Physics A 77 (2003) 163–166.
[24] M.J. Zheng, L.D. Zhang, G.H. Li, X.Y. Zhang, X.F. Wang, Ordered indium-oxide nanowire arrays and their photoluminescence properties, Applied Physics Letters 79 (2001) 839–841.
[25] Q. Tang, W. Zhou, W. Zhang, S. Qu, K. Jiang, W. Yu, Y. Qian, Size-controllable growth of single crystal $In(OH)_3$ and In_2O_3 nanocubes, Crystal Growth and Design 5 (2005) 147–150.
[26] L. Dai, X.L. Chen, J.K. Jian, M. He, T. Zhou, B.Q. Hu, Strong blue photoluminescence from aligned silica nanofibers, Applied Physics A 76 (2003) 625–627.
[27] D.A. Magdas, A. Cremades, J. Piqueras, Growth and luminescence of elongated In_2O_3 micro- and nanostructures in thermally treated InN, Applied Physics Letters 88 (2006) 113107.
[28] X.P. Shen, H.J. Liu, X. Fan, Y. Yuan, J.M. Hong, Z. Xu, Construction and photoluminescence of In_2O_3 nanotube array by CVD-template method, Journal of Crystal Growth 276 (2004) 471–477.
[29] V.I. Arkhipov, P. Heremans, E.V. Emelianova, G.J. Adriaenssens, H. Bassler, Charge carrier mobility in doped semiconducting polymers, Applied Physics Letters 82 (2003) 3245–3247.
[30] E.V. Emelianova, M. van der Auweraer, G.J. Adriaenssens, A. Stesmans, Carrier mobility in two-dimensional disordered hopping systems, Organic Electronics 9 (2008) 129–135.

[31] K. Tsung-Shine, C. Chia-Pu, C. Jun-Rong, L. Tien-Chang, K. Hao-Chung, W. Shing-Chung, Tunable light emissions from thermally evaporated In_2O_3 nanostructures grown at different growth temperatures, Journal of Crystal Growth 310 (2008) 2264–2267.
[32] K.B. Sundaram, G.K. Bhagavat, Preparation and properties of indium oxide films, Physica Status Solidi 63 (2001) K15–K18.
[33] V.E. Henrich, P.A. Cox, The Surface Science and Metal Oxides, Cambridge University Press, Cambridge, 1994.
[34] R. Schaub, E. Wahlstrom, A. Ronnaus, E. Laegsgaard, I. Stensgaard, F. Besenbacher, Oxygen-mediated diffusion of oxygen vacancies on the TiO_2(1 1 0) surface, Science 299 (2003) 377–379.